Research Square

Preprints are preliminary reports that have not undergone peer review.
They should not be considered conclusive, used to inform clinical practice,
or referenced by the media as validated information.

Metagenomic insight into the enhanced biogas production by anaerobic digestion of waste activated sludge with oxygen nanobubble-loaded biochar addition

Cancan Jiang
Research Center for Eco-Environmental Sciences
Huacai Wang
Honghe Hani and Yi Autonomous Prefecture Ecological Environment Bureau
Danhua Wang
Chinese Research Academy of Environmental Sciences
Lei Wang
Research Center for Eco-Environmental Sciences
Xu Wang
wangxu@rcees.ac.cn
Research Center for Eco-Environmental Sciences
Xuliang Zhuang
Institute of Tibetan Plateau Research

Research Article

Keywords: Anaerobic digestion, Waste activated sludge, Oxygen nanobubble, Biochar, Metagenomic

Posted Date: November 25th, 2026

DOI: https://doi.org/10.21203/rs.3.rs-11783062/v1

License: This work is licensed under a Creative Commons Attribution 4.0 International License.
Read Full License

Additional Declarations: No competing interests reported.

Metagenomic insight into the enhanced biogas production by anaerobic digestion of waste activated sludge with oxygen nanobubble-loaded biochar addition

Cancan Jiang[1,2], Huacai Wang[4], Danhua Wang[5], Lei Wang[1,2], Xu Wang[1,2] *, Xuliang Zhuang[3,1,2] *

[1]Research Center for Eco-Environmental Sciences, Chinese Academy of Sciences, Beijing, 100085, China.

[2]College of Resources and Environment, University of Chinese Academy of Sciences, Beijing, 100049, China.

[3]Institute of Tibetan Plateau Research, Chinese Academy of Sciences, Beijing, 100101, China.

[4]Honghe Hani and Yi Autonomous Prefecture Ecological Environment Bureau, Mengzi, 661199, China

[5]State Environmental Protection Key Laboratory of Estuarine and Coastal Environment, Chinese Research Academy of Environmental Science, Beijing, 100012, PR China

*Correspondence and requests for materials should be addressed to X.W. (wangxu@rcees.ac.cn) and X.Z. (Email: xlzhuang@rcees.ac.cn)

Abstract:

Nanobubble is an effective strategy for enhancing anaerobic digestion (AD) of waste activated sludge (WAS), but adding nanobubble water reduces the reaction efficiency by enlarging the AD volume. This study aimed to load oxygen nanobubbles onto sewage sludge biochar (SSBC) to enhance AD by promoting their duration in AD system. SSBC was produced by pyrolysis at 500 °C and loaded with oxygen nanobubbles by vacuum pressurization to obtain oxygen nanobubble-loaded SSBC (ON-SSBC). The oxygen loading capacity of ON-SSBC was 18.42 ± 0.96 mg/g, and a 1% (w/v) ON-SSBC suspension released oxygen nanobubbles with a mean diameter of 163.1 ± 6.2 nm (major diameter around 152 nm) at a concentration of 8.97×10^7 particles/mL. Biochemical methane potential (BMP) tests displayed ON-SSBC addition achieved a methane yield of 145.44 ± 24.23 mL/g VS, corresponding to increases of 4.86 and 3.14 times compared with the control (CK) and the only SSBC group, respectively. The methane yield increment was mainly ascribed to higher SCOD and total EPS generations by 83% and 198% in ON-SSBC relative to SSBC, respectively ($P < 0.01$). Metagenomic analysis indicated that ON-SSBC increased genes encoding key hydrolases (glycosidases and peptidases) and genes involved in short-chain fatty acid generation and consumption compared with CK and SSBC. SSBC mainly enhanced the acetoclastic pathway and *Methanosarcinales*, whereas ON-SSBC also promoted methylotrophic (*Methanosphaera* and *Methanomassiliicoccaceae*) and hydrogenotrophic (*Methanobacterium* and *Methanothermobacter*) pathways. Moreover, ON-SSBC increased genes for F420 biosynthesis and direct interspecies electron transfer, indicated by fewer pili-related genes (*PilA* and *OmcS*) and enrichment of electron-accepting methanogens (*Methanothrix* and *Methanosarcina*).

Keywords: Anaerobic digestion; Waste activated sludge; Oxygen nanobubble; Biochar; Metagenomic

1.Introduction

The worldwide application of activated sludge processes in wastewater treatment plants (WWTPs) has greatly reduced water pollution and contributed to a better and healthier living environment for human beings (Wang et al., 2019b). However, large amounts of waste activated sludge (WAS) are simultaneously produced as the solid byproduct, and improper disposal of WAS can cause

severe environmental impacts and health hazards (Hao et al., 2020). Consequently, WAS treatment has become a global public challenge, and numerous approaches have been proposed (Xu et al., 2020a). Among them, anaerobic digestion (AD) is regarded as an attractive and promising method because of its advantages in sludge reduction, biogas recovery, and operation costs(Zhen et al., 2017). AD is a series of microbial conversion processes that occur under anaerobic conditions and mainly involve four stages: hydrolysis, acidogenesis, acetogenesis, and methanogenesis (Campanaro et al., 2018; Choi et al., 2018). WAS is a complex mixture of microbial cells, organic and inorganic compounds, and extracellular polymeric substances (EPS) that are resistant to disruption and decomposition. As a result, the hydrolysis rate of WAS is usually low, and hydrolysis is widely recognized as the rate-limiting step in AD. In addition, AD performance is further limited by inhibition from intermediates and by inefficient syntrophic interactions and interspecies electron transfer between fermenting bacteria and methanogens. Therefore, AD of WAS without enhancement measures is usually unsatisfactory (Kor-Bicakci and Eskicioglu, 2019; Wei et al., 2018).

To improve biogas production, various AD enhancement methods have been proposed, including ultrasound, thermal treatment, and additive supplementation (Chuenchart et al., 2021; Liu et al., 2021; Wang et al., 2019a; Wang et al., 2020b). Nanobubble application has attracted increasing attention as a novel strategy for enhancing anaerobic digestion (AD). Nanobubbles are typically defined as gas bubbles with a diameter <1 μm. Since their existence was first evidenced by tapping-mode atomic force microscopy, nanobubbles have attracted considerable interest, and successful applications have been reported in medicine, physiology, and water treatment (Agarwal et al., 2011; Brenner and Lohse, 2008; Ebina et al., 2013). In the context of AD, nanobubbles are considered to enhance biogas yield mainly due to the high gas-liquid interfacial area and ability to generate free radicals in aqueous solution (Lou et al., 2000; Ohgaki et al., 2010; Temesgen et al., 2017). However, the microbial and genetic mechanisms underlying nanobubble enhanced AD remain insufficiently understood.

Nanobubbles are generally categorized into two types (Yang et al., 2019). The first type is bulk nanobubbles dispersed in bulk liquids and applied as nanobubble water (NBW), such as O_2 and N_2 NBWs (Felden et al., 2010). Although NBW addition has been reported to enhance biogas yield during AD (Fan et al., 2020; Wang et al., 2020d), this approach increases the liquid the AD

system volume and dilutes the substrate, potentially offsetting the expected benefits. The second nanobubble type is surface nanobubbles, which are nanoscopic gaseous domains at solid-liquid interfaces (Gantzer et al., 2009; Shi et al., 2018). Unlike NBW addition, which increases the liquid volume and dilutes the substrate, surface nanobubbles are retained enduringly at the interfaces of porous solid particles rather than dispersed in the bulk liquid and may therefore alleviate this trade-off (Lohse and Zhang, 2015; Weijs and Lohse, 2013). In our previous work, activated carbon or biochar exhibited higher oxygen nanobubble loading capacities than other porous particles, including diatomite, zeolite, coal ash, and clay (Wang et al., 2018b). Thus, biochar may be a promising carrier for delivering nanobubbles into fermentative systems to enhance AD performance.

It is worth noting that biochar has also been increasingly investigated as an efficient additive for AD enhancement in recent years (Luo et al., 2015; Singh et al., 2020). Biochar is generally produced by pyrolysis of carbon-rich biomass residues, such as crop residues and sewage sludge, under oxygen-limited conditions (Tang et al., 2019). Previous studies have demonstrated that biochar can adsorb microbial inhibitors and promote the adhesion of methanogenic consortia owing to its rich surface functional groups and porous structure (Wu et al., 2019; Zhang et al., 2019b). In addition, biochar can facilitate electrical connections in syntrophic metabolism by promoting direct interspecies electron transfer (DIET) because of its conductive and redox-active properties (Chen et al., 2014; Zhang et al., 2018b). These properties, together with its capacity to carry nanobubbles, make biochar a promising external accelerator for improving AD performance. Nevertheless, whether oxygen nanobubbles can be effectively loaded onto biochar and whether the resulting composite can enhance biogas production during AD of WAS remain unclear.

This study therefore investigates the feasibility of loading oxygen nanobubbles onto biochar and the enhancement of biogas production during AD of WAS. Specifically, the biochar used in this study was derived from waste sewage sludge via pyrolysis, which not only reduces the sludge volume requiring disposal but also lowers the cost associated with external biochar supplementation. The properties of sewage sludge biochar (SSBC) and oxygen nanobubbles loaded on SSBC (ON-SSBC) were first characterized. The effects of ON-SSBC addition on the solubilization and hydrolysis of WAS were then evaluated in terms of short-chain fatty acids (SCFA) and biogas yield. Finally, the enhancement of biogas production by ON-SSBC and the

associated microbial mechanisms were investigated using biochemical methane potential (BMP) tests and metagenomic sequencing. This study is expected to provide a mechanistic and practical basis for developing low cost biochar-based nanobubble additives, thereby supporting sustainable WAS reduction and biogas recovery.

2.Materials and methods

2.1. Preparation of SSBC

Sewage sludge (SS) used for biochar preparation in this study was dewatered WAS from a spiral centrifugal dehydrator in a WWTP (Beijing, China). The sludge was air dried and heated in an oven (105 °C) to remove water content before pyrolysis in a tubular furnace. The heating procedure started from 30 °C with a heating rate of 5 °C/min to a desired final temperature of 500 °C for 2 h. Nitrogen gas (99.99%, v/v) was injected at a flow rate of 200 mL/min to ensure an oxygen-free environment throughout the whole process. The pyrolysis temperature was selected based on previous studies that indicated the biochar produced between 500 and 600 °C exhibited preferable physiochemical properties (e.g., surface area, porosity and bioelectrical charge) (Pan et al., 2019; Zhang et al., 2020; Zhou et al., 2020). The obtained biochar samples were ground and sieved to $<$0.3mm sized particles. To remove impurities such as ash, all samples were rinsed in distilled water until pH remained constant and dried at 105 °C for characterization and following uses.

2.2. Characterization of SSBC

Electrical conductivity (EC) and pH of the produced SSBC were determined with a MultiLine® Multi 3630 IDS (WTW Company, Germany) by adding SSBC to deionized water with a ratio of 1:5 (w/v) and then shaking for 1.5 h at 200 rpm (Wu et al., 2019). The specific surface area and pore size distribution of SSBC were determined from low-temperature (77.3 K) nitrogen adsorption desorption isotherms obtained from an ASAP 2460 surface area and porosity analyzer (Micromeritics, USA). Before analyzing, the samples were degassed at a temperature of 200 °C under vacuum for 48 h. Surface morphology and the relative element content of SSBC were investigated using a field emission scanning electron microscopy (FE-SEM) equipped with an energy-dispersive X-ray spectroscopy (EDS) (Bruker Nano GmbH Berlin, Germany).

150

151 **2.3. Load of oxygen nanobubbles on SSBC**

152 Oxygen nanobubbles were loaded on SSBC using the vacuum pressurization method modified
153 according to our previously reports (Shi et al., 2018; Wang et al., 2018b; Zhang et al., 2018a).
154 First, the gas in the pores of the SSBC was removed by evacuating for 2 h under pressure of -0.08
155 MPa in an airtight container. Pure oxygen (99.999%) was then added into the container and held at
156 a pressure of 0.12 MPa for 4 h to load the O_2. To achieve supersaturation of O_2 in the SSBC pores,
157 the evacuation and oxygen loading processes were repeated for three times and the oxygen
158 pressure was then kept at 0.12 MPa pressure for 12 h before reducing to atmospheric pressure. The
159 ON-SSBC were prepared freshly before use.

160

161 **2.4. Characterization of oxygen nanobubbles releasing from ON-SSBC**

162 Oxygen loading capacity of SSBC was measured according to the method in previous reports (Shi
163 et al., 2018; Wang et al., 2018b). The analysis system consisted of two connected sealed cells
164 including oxygen release cell (ORC) and oxygen absorption cell (OAC), respectively. The ORC
165 was filled with oxygen-free water and used for oxygen release from SSBC. The OAC was filled
166 with the Na_2SO_3 solution of known concentration for oxygen adsorption. A certain amount of ON-
167 SSBC were placed into the ORC and the released oxygen was transferred into the OAC by pure
168 N_2 (99.999%). The amount of oxygen loaded on SSBC was obtained by measuring the changes of
169 Na_2SO_3. To investigate the effect of air exposure time on oxygen releasing capacity of ON-SSBC,
170 the quality of oxygen released from ON-SSBC as exposure in the air (10s, 20s, 40s, 1min, 5min,
171 10min, 20min, 40min, and 1 hour) were measured. Concentration and size distribution of
172 nanobubbles released from ON-SSBC were measured in a 1% (w/v) ON-SSBC/distillate water
173 suspension with a nanoparticle-tracking analysis instrument (NanoSight NS500 & NTA 2.0
174 Analytical Software, Malvern Instrument Ltd., Salisbury, UK) at room temperature (25 ± 1 °C).

175 **2.5. Pretreatment of WAS by ON-SSBC before AD**

176 Three test groups were set to evaluate the effect of ON-SSBC addition on WAS before AD,
177 including no additives addition group, SSBC addition group, and ON-SSBC addition group, and
178 were labelled as CK, SSBC, and ON-SSBC, respectively. In the ON-SSBC group, 2 g ON-SSBC
179 were added into a 250 mL bottle with 200 mL substrate sludge in it. To minimize the loss of

oxygen loaded on SSBC and to ensure uniformity across treatments, the ON-SSBC were added into the substrate sludge 10s after prepared, as determinated in Section 2.4. And then, the bottle was placed in a constant temperature incubator (37 °C) for 24 hours before BMP test. In the other two groups, pretreatment processes were identical with ON-SSBC group except that no additives were added in CK group and 2 g SSBC were added in SSBC group. The experiments in the three groups were repeated in triplicate. After the pretreatment process, three kinds of EPS, including soluble EPS (S-EPS), loosely bound EPS (LB-EPS), and tightly bound EPS (TB-EPS), were extracted and compared with that of substrate sludge before pretreatment. The method used in this study was modified based on previous literatures (Guo et al., 2020; Liu and Fang, 2002). 10 ml of substrate sludge or pretreated sludge were first centrifuged at 6000 rpm, 4°C for 10 min, and then the supernatant was filtered through a 0.45 μm filter membrane and gathered as S-EPS. The residual sample was resuspended by 0.05 % NaCl solution to the original volume and heated in a water bath for 10 min under 70 °C before centrifuged at 6000 rpm 4°C for 10 min, and the supernatant was gathered as LB-EPS after filter through a 0.45 μm filter membrane. And then, the residual sample was resuspended again by 0.05 % NaCl solution to the original volume and heated in a water bath for 30 min under 80 °C before centrifuged at 6000 rpm, 4°C for 15 min, and the supernatant was gathered as TB-EPS after filter through a 0.45 μm filter membrane. Proteins were determined by the modified Lowry method using casein as the standard. Polysaccharide was measured by Anthrone-H_2SO_4 colorimetry with glucose as the standard (Wu et al., 2020a; Yu et al., 2008).

2.6 Biogas production test

2.6.1. Substrate and inoculum

The substrate sludge was collected in the secondary settler of the same WWTP described in Section 2.1. The sludge was stored in a refrigerator at 4 °C before use. The inoculum sludge was taken from a 10 L anaerobic reactor with long-term stable operation at 37°C in our laboratory. The main characteristics of substrate sludge and inoculum sludge were listed in Table S1.

2.6.2. BMP test

Batch AD experiments were conducted in an AMPTS II system (Bioprocess Control, Sweden) according to the protocol of BMP tests. The system has a total of 9 identical Schott glass bottles used as anaerobic digesters and for the three test groups mentioned above (CK, SSBC, ON-

SSBC), 150 ml substrate sludge and 150 ml inoculum sludge were added in each bottle with a volatile solids (VS) ratio of 1:1.2. Before startup, each digester was degassed with high-purity N_2 (99.999%) for 5 min to obtain anaerobic condition. The temperature was maintained at 37 ± 1 °C and the agitation speed was controlled at 120 rpm throughout the experiment. The gas outlet of each digester was first connected to an airtight bottle containing 3 M NaOH solution for CO_2 sequestration. Subsequently, the volume of CH_4 produced from each digester was measured and recorded by a real-time gas measurement unit. All the gas volume production data was reported at STP condition (273 K, 1 atm).

2.7 Sampling and DNA extraction

Samples collected in this study included initial mixed sludge in triplicate before AD and digested sludge from each bottle in the three experiment groups (CK, SSBC, ON-SSBC) at the middle (day 8) and at the end of BMP tests (day 16). 0.5 mL of each sample was used for DNA extraction using a FastDNA SPIN Kit for soil (MP Biomedicals, USA) following the manufacturer's instructions. The concentration and quality of DNA were measured using a Micro-Volume UV-Vis Spectrophotometer (NanoDrop ND-1000, Thermo Scientific, USA). The DNA samples were stored at -20 ℃ for further analysis.

2.8 Metagenomic sequencing analysis and bioinformatic analysis

The triplicate DNA extracts of the same group were composited to get a representative DNA sample. Metagenomic sequencing was conducted at the Majorbio Bio-Pharm Technology Co., Ltd. (Shanghai, China). DNA extract was sheared into around 400 bp fragments using Covaris M220 (Gene Company Limited, China) for paired-end library construction with NEXTFLEX Rapid DNA-Seq (Bioo Scientific, Austin, TX, USA). Adapters containing the full complement of sequencing primer hybridization sites were ligated to the blunt-end of fragments. Paired-end sequencing (2 × 400 bases) was performed on Hiseq 4000 (Illumina) using NovaSeq Reagent Kits/HiSeq X Reagent Kits according to the manufacturer’s instructions. Adapters trimming and removal of low-quality reads (length<50 bp or with a quality value <20 or having N bases) were performed using fastp. The clean reads were assembled using Multiple_Megahit. Open reading frames (ORFs) from each assembled contig ≥300 bp were predicted using MetaGene. The predicted ORFs with length ≥100 bp were retrieved and translated into amino acid sequences using the NCBI translation table.

A non-redundant gene catalog was constructed using CD-HIT with 90% sequence identity and 90% coverage. Reads after quality control were mapped to the non-redundant gene catalog with 95% identity using SOAPaligner, and gene abundance in each sample were evaluated by TPM. Sequences of non-redundant gene catalog were aligned to NCBI NR and Kyoto Encyclopedia of Genes and Genomes (KEGG) database with e-value cutoff of $1e^{-5}$ using BLASTP (Version 2.2.28 +) for taxonomic and functional annotations.

2.9 Statistical analysis

Taxonomic and functional data were analyzed on the online platform of Majorbio Cloud Platform (https://cloud.majorbio.com/). To assess the influence of different anaerobic digestion conditions on the microbiology richness and diversity, the alpha diversity indices (Observed richness, Pielou evenness, Shannon and invSimpson indices) were calculated based on the results of taxonomic annotations. Principal component analysis (PCA) was further performed to evaluate the profiles of microbial communities in different treatments. For statistics comparison between two samples, chi-square test t was used and a significant difference was considered when *P* value was below 0.001.

3. Results and discussion

3.1. Characteristics of produced SSBC and released oxygen nanobubbles

The surface morphology and main characteristics of SSBC produced in this study are shown in Fig. 1A and Table S2. As showed in the FE-SEM picture (Fig. 1A), the SSBC was a porous structure with plenty of pores in both surface and interior, pore diameters of which arranged from nanometer to micrometer with an average pore diameter of 18.95 nm (Table S2). The pore diameters were similar with SSBCs produced in previous articles, which ranged from 10.76 to 21.3 nm (Wu et al., 2019; Zhang et al., 2019a). The BET surface area and electrical conductivity (EC) of the produced SSBC under the pyrolysis temperature of 500 °C were 7.52 m^2/g and 1.5 Ds/m. It was reported that the surface and EC of SSBC subsequently increase until the pyrolysis temperature reaches 500 °C and could reduce greatly as pyrolysis temperature rises (Figueiredo et al., 2017; Lu et al., 2013; Singh et al., 2020) . A larger surface area is usually contributing to larger oxygen-loading capacity (Wang et al., 2018b) and a higher EC is benefit to electron transfer between methanogens (Fagbohungbe et al., 2017; Lu et al., 2014), which might both facilitate the

AD performance of WAS.

The diameter, concentration and sample video frame of oxygen nanobubbles released from ON-SSBC were detected in the water solution with ON-SSBC addition. As shown in Fig. 1A, the mean diameters of nanobubbles released from ON-SSBC were 163.1±6.2 nm, with a major particle diameter around 152 nm. The average concentration of nanobubbles released by ON-SSBC was 8.97×10^7 particles/mL, which were approximate to that produced by nanobubble generators (Haris et al., 2020; Wang et al., 2019a; Yang et al., 2019). When analyzed combined with the SSBC characteristics, there are several reasons might explain the excellent performance of ON-SSBC on generating nanobubbles. Firstly, the large number of micro-mesopores in the surface and interior played a key role in the enhancement of nanobubble production, which also determined the size of released nanobubbles (Xie et al., 2012). Secondly, the abundance in element composition of SSBC produced in this research was also an important promoter for the generation of nanobubbles (Tan et al., 2020; Xie et al., 2012). Last but not the least, it was reported that the rich functional groups on the surface of SSBC could facilitate adherence of oxygen and hence boost nanobubble production (Ulatowski and Sobieszuk, 2020). To investigate the effect of air exposure time on oxygen releasing capacity of ON-SSBC produced by the vacuum-pressurization method used in this study, the quality of oxygen released from ON-SSBC as exposure in the air (from 10s to 1 hour) were measured (Fig. 1B). The results showed that 18.42 ± 0.96 mg/g oxygen could release from ON-SSBC after exposure in the air for 10s. The amount reduced by 45.17% in the first minute and by 81.70% in the following experiment period. Therefore, to minimize the loss of oxygen loaded on SSBC, the ON-SSBC were added into the substrate sludge within 10s after taken out from the airtight container.

Fig.1 Nanobubble concentrations and size distribution in water solution with 1% (w/v) ON-SSB Caddition, SEM picture of produced SSBC (above) and sample video frame of nanobubbles released from ON-SSBC (below) (A) and effect of air exposure time on oxygen releasing capacity of ON-SSBC (B).

3.2 Effects of ON-SSBC addition on solubilization and hydrolysis of WAS

The complex microstructure and components make WAS especially difficult to hydrolyze. To

investigate the effects of ON-SSBC addition (24 hours before AD) on solubilization and hydrolysis of WAS, two of the most relevant parameters (SCOD and EPS) were detected and compared (Fig. 2). The results showed that SCOD and total EPS content in CK after incubation under 37 °C for 24 hours before AD increased from 495±54 and 54.56±3.04 mg/g VS to 1183±172and 67.58 ± 0.98 mg/g VS, respectively (Fig. 2A). This phenomenon was also reported in other researches that during pretreatment of WAS under mesophilic or thermal condition, hydrolytic microorganisms depolymerized sludge cell EPS network and microbial cell walls and resulted in the release of smaller dissolved compounds (Ding et al., 2017; Kavitha et al., 2014). The addition of SSBC promoted the solubilization degree of organic matter in WAS in this study, which was also in accordance with previous reports that attribute it to the enhancement of hydrolase activity and improvement of digester buffering capability stemming from biochar's alkalinity (Lü et al., 2020; Wu et al., 2019). After loaded with nanobubbles, the ability of SSBC to enhance solubilization and hydrolysis of WAS was further improved. SCOD and total EPS contents increased by 83% and 198%, respectively, compared to that of SSBC (Fig. 2A).

EPS is generally considered as a protective shield and prevent the sludge cells rupture and lysis, and thereby blocks the disintegration and solubilization of WAS (Wu et al., 2020a; Yu et al., 2008). The outer-to-inner three-dimensional, gel-like structure of EPS was composed of slime EPS (S-EPS), loosely bound EPS (LB-EPS), and tightly bound EPS (TB-EPS). Proteins (PN) and polysaccharides (PS)are two of the most predominant organic matters in EPS, which account for 70-80% of the total organic carbon (Liu et al., 2020). Therefore, the variations in PN and PS in different layers of EPS were also detected to gain an insight into the distribution and migration of EPS upon ON-SSBC pretreatment and to provide a more thorough understanding of subsequent influences on AD process (Fig. 2B, 2C). In substrate sludge, the contents of PN and PS were 31.99±1.98 and 19.25±0.59 mg/g VS, which were both predominant in TB-EPS layers, with a percentage of 56.08% and 66.60%, respectively. After pretreatment of incubation under 37 °C for 24 hours without any additives (CK), PN were transferred from TB-EPS to LB-EPS and S-EPS slightly. With the addition of SSBC and ON-SSBC, this transference was further enhanced. Especially for ON-SSBC, the PN contents of which in S-EPS was dominant in the three layers (70.46%) (Fig. 2B). Similar variation tendency can be observed in PS contents that significantly increased to 18.85 ± 0.21 mg/g VS (61.16%) in S-EPS in group ON-SSBC from 5.38 ± 0.21 mg/g

VS (23.86%, CK) and 6.36 ± 0.21 mg/g VS (24.30%, SSBC), respectively (P<0.05) (Fig. 2C). The distribution and migration of PN and PS in different layers indicated that ON-SSBC addition could cause organic matters transform from tightly bound fractions to loosely bound fractions and slime layer as a result of disruption and solubilization of microbial cells and EPS (Xiao et al., 2020; Yu et al., 2008). There are some potential mechanisms that might explain the excellent solubilization and hydrolysis effect on WAS under ON-SSBC addition. Firstly, a mass of oxygen brought into the reaction system by ON-SSBC created an aerobic environment and gradually transformed into a microaerobic environment, which greatly promote the hydrolysis of macromolecular substance (Khanh Nguyen et al., 2021; Liu et al., 2013; Nguyen et al., 2019; Xu et al., 2018). Secondly, it is reported that plenty of free radicals could produce upon the collapse of nanobubbles which might lead to disruption of sludge cells and provoke the release of more EPS and intracellular polymeric substances into the liquid (Xu et al., 2020b; Yang et al., 2019; Zhen et al., 2017). The excellent sludge cells disruption ability of ON-SSBC could also be confirmed by the significant increase of DNA proportion in EPS from 8.39% (SSBC) to 12.62% (ON-SSBC) (P<0.01) (Fig. 2D), since the DNA content of EPS usually regards as a good marker of cell disruption (Kavitha et al., 2014; Yu et al., 2008).

Fig.2 Effects of ON-SSBC addition on SCOD release (A) and EPS distribution and migration (B for protein, C for polysaccharide and D for DNA)

3.3 Enhancement of ON-SSBC on biogas production

The BMP tests were carried out to evaluate the impacts of ON-SSBC addition on biogas production during AD of WAS. The results are shown in Fig. 3. After 24 hours pretreatment with SSBC addition and the following 16 days AD at 37 ℃, the total methane production was 35.11 ± 6.43 mL/g VS in SSBC group, increased by 41.29% in comparison to the group without any additives (CK). The present result was in accordance with previous findings that an increase in methane production was observed as biochar was added in the sludge AD system (Shen et al., 2021; Zhang et al., 2019b). For example, the increasing rates of 26.2%, 48.3%, and 120% were reported in other researches as corn biochar, Douglas fir biochar, and sludge biochar were used

(Wang et al., 2020b; Wu et al., 2019; Zhou et al., 2020). It is reported that the stimulatory impact of biochar on methane production is more associated with the acetogenic-methanogenic stages rather than the hydrolysis-acidogenesis steps during AD of WAS (Shen et al., 2021). Firstly, the porous structure of biochar promotes rapid formation of biofilms by enrichment of methanogens, thereby enhancing their synergy and activity (Cooney et al., 2016; Yan et al., 2020). Secondly, biochar is added as conductive material and enhances DIET during AD process (Chen et al., 2020; Wu et al., 2020b). As the oxygen nanobubbles loaded biochar was added, the methane production in ON-SSBC group was improved enormously to 145.44 ± 24.23 mL/g VS, increased by 3.14 times compared with that of SSBC group. This indicated that the synergistic effects of released oxygen nanobubbles (mainly promoted the solubilization and hydrolysis of WAS) and SSBC (mainly facilitated methanogenesis) extremely promoted the methane production during AD of WAS.

Fig.3 Total methane production during anaerobic digestion in different groups.

3.4 ON-SSBC addition reshapes the microbial community and enriches functional taxa in AD of WAS

To investigate the underlying microbial mechanisms involved in the enhancement of biogas production during the AD of WAS under ON-SSBC addition, the whole microbial community in the initial mixed sludge before AD (MS) and in sludge from different samples (CK8, SSBC8, ON-SSBC8, CK16, SSBC16, ON-SSBC16) were analyzed by metagenomic shotgun sequencing. A total of 7498890 gene sequences were predicted, and 2323292 non-redundant gene catalogs were constructed from the 7 sequenced samples. In specific, 4543 genera and 30198 species were annotated. Alpha diversity based on the observed richness index showed a general increase in whole microbial community richness of the digested sludge in CK, SSBC and ON-SSBC compared to MS (Fig. 4A). However, AD treatment of WAS cased negative effects on community evenness and diversity, which indicated by decline of Pielou evenness index, Shannon index, and InvSimpson index. Notably, SSBC had a higher community richness, evenness and diversity than CK, while ON-SSBC possessed the lowest values of theses indexes among the digested samples

on both Day 8 and Day16. The alpha diversity of bacterial community in different groups exhibited a similar tendency with the whole microbial community (Fig. S1A), while an obvious dissimilarity could be observed in archaeal community, that the ON-SSBC groups had a comparable or higher Pielou evenness index, Shannon index, and InvSimpson index, as compared to SSBC groups (Fig. S2A). The possible explanation could be that biochar addition in SSBC groups diversified the microbial community by indiscriminatingly enriching fermentation microflora and posing little inhibitory effect on other microorganisms (Kumar et al., 2021; Luo et al., 2015; Zhao et al., 2021). Similar results were reported in previous studies which indicated that moderate addition of biochar could increase the richness and diversity of microbial communities compared to treatments without biochar (Lim et al., 2020; Wang et al., 2018a). In the ON-SSBC group, although certain anaerobic digestion-related microbes and methanogenic archaea that resulted in higher methane yield could be enriched by the microoxygen environment created by oxygen nanobubble and biochar, nanobubbles released from ON-SSBC lysed microbial cells and inhibited some other species (Chuenchart et al., 2021; Wang et al., 2020d).

Fig. 4 Alpha diversities of microbial communities (A) and principal component analysis (PCA) of the whole microbial community on species level (B) of sludge samples from different groups

Results of principal component analysis (PCA) also indicated the significant difference in the enrichment and inhibitory effect of SSBC and ON-SSBC on microbial communities. For the whole microbial communities, the first component (PC1) and the second component (PC2) accounted for 36.81% and 18.63% of the total variation, respectively. Samples from CK and SSBC group clustered into the same quadrants according to the fermentation time, while samples of different fermentation time in ON-SSBC group clustered into a same quadrant (Fig. 4B). It indicated that the addition of ON-SSBC caused a greater variation in microbial community structure. For the archaea community, a similar result could be observed that samples from ON-SSBC clustered into a quadrant and samples from CK and SSBC groups clustered into the other quadrant (Fig.S2B). However, for the bacterial community, the effects of ON-SSBC addition on the community structure are less clear indicated by indistinct separation between samples from

ON-SSBC group and samples from CK or SSBC group (Fig.S1B). The PCA result suggested that the variation in archaeal community structure was higher than in bacterial community with the ON-SSBC addition.

To further investigated the response of microbial communities to ON-SSBC addition, the microbial compositions at different classification levels were analyzed. As showed in the Circos plot (Fig.S3), *Proteobacteria*, *Chloroflexi*, *Bacteroidetes* and *Actinobacteria* were the predominant phyla in all groups. Among them, *Proteobacteria* was enriched and the others decreased or maintained in SSBC on both Day 8 and Day 16 as compared with that of CK from the same day. However, distinct results were gained in ON-SSBC that *Proteobacteria* dropped obviously from 39.74% (CK8) and 34.95% (CK16) to 31.21% (ON-SSBC8) and 24.85% (ON-SSBC16), respectively, while the other phyla apparently increased as compared with CK from the same sampling time. A similar phenomenon could also be observed from the heatmap at the species level that a majority of species belongs to *Proteobacteria* were dramatically inhibited, and species belong to *Chloroflexi*, *Bacteroidetes* and *Actinobacteria* were markedly enriched in ON-SSBC group on Day 8 and Day 16 when compared with CK or SSBC group (Fig. 5). Specifically, of the top 100 species annotated, 10 species increased significantly and 15 species decreased significantly on Day 8, and these numbers changed to 14 and 22 on Day 16, respectively, as compared with SSBC from the same sampling day (P<0.001). Microorganisms enriched in ON-SSBC groups that contribute to enhancement of AD of WAS can be divided into three groups. The first groups were bacteria that facilitated degradation and hydrolysis of recalcitrant compounds and complex molecules (protein and polysaccharide, etc.) that transformed to S-EPS during the pretreatment process to simple monomers (amino acids and glucose, etc.) (Li et al., 2019; Wang and Lee, 2021). The representatives were *Firmicutes bacterium* ADurb.Bin153 and *Clostridiales bacterium* that belongs to phyla *Firmicutes*, and *Bacteroidales bacterium* that belongs to phyla *Bacteroidetes* (Beraud-Martinez et al., 2021; Narihiro et al., 2015). The enrichment of hydrolytic bacteria, which can be promoted by low-oxygen range micro-aeration, might be contributed from the microaerobic environment induced by oxygen nanobubbles released from ON-SSBC (Fu et al., 2016; Guo et al., 2021). It is reported that the microaerobic condition created by NB, with an oxidation-reduction potential (ORP) range of 0 to −412 mV, is within the ORP range (0 to −470 mV) for an optimal AD process (Hou et al., 2021a; Nguyen and Khanal, 2018; Wang et al., 2021).

The second groups were hydrogenotrophic and methylotrophic methanogens that can enhance methane production by utilizing H_2/CO_2 and methyl compounds as substrates (Fig. S4). The representatives were *Methanobacterium*, *Methanothermobacter*, *Methanosphaera* that belongs to order *Methanobacteriales*, and *Methanosphaerula*, *Methanofollis* that belongs to order *Methanomicrobiales* (Narihiro and Sekiguchi, 2007; Tian et al., 2017). Noticeably, ON-SSBC might also promote methanogenesis by enhancing DIET, which was indicated by the enrichment of electron accepting methanogens (*Methanothrix* and *Methanosarcina*) (Rotaru et al., 2014; Wang and Lee, 2021).

Fig.5. The heat map showing the top 100 bacterial species in each sample. The green triangle and pentagram represented the significant decrease of corresponding species in ON-SSBC compared with SSBC on day 8 and day 16, respectively. The red triangle and pentagram represented the significant increase of corresponding species in ON-SSBC compared with SSBC on day 8 and day 16, respectively. (Chi-squaretest,$P < 0.001$)

3.5 ON-SSBC addition enhances key hydrolysis–acidogenesis–acetogenesis genes and SCFA turnover

To further understand and exploit the impact of ON-SSBC addition on microbial metabolism, the abundance of genes that encoded the key enzymes for main processes of anaerobic digestion (hydrolysis, acidogenesis, acetogenesis, and methanogenesis) were investigated in the KEGG database and summarized in Fig. 6. The following discussion first addresses hydrolysis-related genes and then moves to acidogenesis- and acetogenesis-related genes and the associated SCFA turnover.

At the hydrolysis stage, as depicted in Fig. 6A, the total abundance of genes that encoded key genes of hydrolases involved in polymeric organic matter degradation, including esterases (EC 3.1), glycosidases (EC 3.2), and peptidases (EC 3.4), increased obviously in ON-SSBC compared to CK and SSBC, especially for glycosidases and peptidases. Furthermore, the abundance gap of these hydrolases between ON-SSBC and CK/SSBC became wider as fermentation time increased from 8 days to 16 days. The increase of hydrolases related genes suggested that the degradation of refractory substrates (protein and polysaccharide, etc.) that released from disrupted sludge cells

and EPS matrix were enhanced. Similar results were reported in previous studies that hydrolysis rate and the activities of extracellular hydrolases (α-glucosidase and protease, etc.) were improved during AD of WAS with NBW addition (Hou et al., 2021a; Hou et al., 2021b). Researchers also found that decomposition of cellulose and lignin and the related enzyme activity were significantly enhanced with NBW addition in the AD system (Chuenchart et al., 2021; Wang et al., 2020c; Wang et al., 2020d). The possible mechanism might be that the microaerobic environment created by NBs released from ON-SSBC promoted the activity and diversity of hydrolysis bacteria such as *Firmicutes* and *Bacteroidales* as analyzed previously, which are mainly associated with degrading lignocellulosic biomass (Chuenchart et al., 2021; Wang et al., 2020c). Moreover, long lifespan of oxygen NBs in aqueous solution can contribute to a continuous microaerobic environment which can not only benefit hydrolysis consistently, but also promote syntrophic interactions among different microbial groups, thereby creating a more stable process (Nguyen and Khanal, 2018; Ruan et al., 2019).

The hydrolysis products, mainly monosaccharides and glycerol, are then converted through acidogenesis and acetogenesis following hydrolysis. These pathways of acidification and acetogenesis mainly consist of pyruvate formation from hydrolysis products (monosaccharides and glycerol), pyruvate and fatty acids transformations toward SCFAs (acetate excepted), amino acids transformation, and further oxidation of nongaseous products of acidogenesis toward acetate and H_2/CO_2 (Amani et al., 2010; Carabeo-Pérez et al., 2019). It could be noticed that the addition of SSBC enhanced pyruvate formation from monosaccharides and glycerol (Fig. 6B), which was agreed with previous studies that used biochar for enhancing biogas production from AD (Khalid et al., 2021; Kumar et al., 2021). The addition of ON-SSBC further promoted this process and the following formation of SCFAs (acetate excepted) from pyruvate and acetyl-CoA (Fig. 6B). It is worth noting that the genes related to acetate formation from acetate/acetyl-CoA, amino acids and SCFAs (acetate excepted) were not enrich by ON-SSBC compared to SSBC, while the genes related to H_2/CO_2 formation were increased largely. The results indicated that the processes of VFAs generation (acetate excepted) and consumption (acetate included) were both enhanced. Similarly, Hou et al.(Hou et al., 2021a) observed that higher total VFAs production and the following hydrogen yield from VFAs were achieved with Air-NBW addition, which both depended chiefly on the increase of butyric acid rather than acetic acid. The underlying causes are

proposed as follows. Firstly, microaerobic environment created by oxygen NBs promoted facultative bacterial (enzymes and genes) that generated VFAs by degradation of hydrolysis products (Fan et al., 2020). Meanwhile, the microaerobic environment inhibited bacteria, biochemical reactions and related genes that rely on anaerobic environment to form acetate. For example, glycine reductase (EC: 1.21.4.2) and sarcosine reductase (EC: 1.21.4.3) associated with Sickland reaction that ferment amino acids to acetate (Fig. 6B) were reduced and the abundance of *Spirochaetae* that transfer of VFAs to acetate was decreased with ON-SSBC addition (Fig. 4). Secondly, the high specific surface area of NBs, improved mobility of water molecules by NBs resealed from ON-SSBC, and accelerated supply of nutrients and trace elements by the hydrophilicity of NB surface, jointly promoted the consumption of VFAs (Temesgen et al., 2017).

Fig.6 Metabolic pathways related to hydrolysis (A), acidogenesis & Acetogenesis (B), and methanogenesis (C). 1~29 represented the reaction of corresponding pathways and abundance information of related enzymes (heatmap); bar chart represented the total abundance of enzymes for corresponding pathways.

3.6 ON-SSBC addition shifts methanogenic pathway partitioning and electron-transfer strategy to enhance methane production

Three mainly recognized methanogenic pathways, including acetoclastic (M00357), hydrogenotrophic (M00567) and methylotrophic pathway (M00356 and M00563), were profiled and depicted in Fig. 6C. The total abundance of all the modules in ON-SSBC was the highest among the groups from the same day, which was in accordance with the highest methane yield in ON-SSBC as discussed previously. A common multiplication of the related methanogens and genes occurred in the three methanogenic pathways from day 8 to day 16, indicated by the obvious rise in abundance of corresponding modules. While the acetoclastic pathways had always been the primary approach to achieve methanogenesis, which was consist with previous studies about AD of WAS (Duan et al., 2021; Ma et al., 2021; Zhao et al., 2020). It is surprising that methylotrophic pathways, including methanol methanogenesis (M00356) and methylamine/dimethylamine/trimethylamine methanogenesis (M00563), were the second dominant methanogenesis, with the abundance > 30% of all the modules related to

methanogenesis. Its abundances in previous studies were usually less than 10% (Xing and Wang, 2021; Zhang et al., 2021). This unusually high abundance of methylotrophic modules prompted a closer examination of the methylotrophic and hydrogenotrophic pathways under ON-SSBC addition.

With the addition of ON-SSBC, the related genes in methylotrophic pathways that encoded methyl-compound methyltransferases and corrinoid protein, i.e., Mta, Mtm, Mtb, and Mtt, were commonly enriched (except for *mtaA*) compared with CK or SSBC. The enhancement of methylotrophic pathway with addition was consistent with the enrichment of H_2-dependent methylotrophic methanogens such as *Methanosphaera* and Methanomassiliicoccaceae (Fig.S4). Wang et al (Wang et al., 2020d) reported that Air-NBW and O_2-NBW can enrich methylotrophic methanogens (*Methanomassiliicoccus*) utilizing H_2 and methanol or methylamines as substrates and enhance methane production. It is reported that the abundance of *Methanomassiliicoccaceae* increases by addition of hydrogen in anaerobic reactor which might be achieved by the enrichment of H_2 formation related genes with ON-SSBC addition in this study (Beraud-Martinez et al., 2021; Treu et al., 2019) (Fig. 6B). For hydrogenotrophic pathway, the abundance of genes that encoded the key enzymes for reduction of CO_2 to CH_4 with ON-SSBC addition were higher than that of CK or SSBC, which include formylmethanofuran dehydrogenase (EC: 1.2.7.12), formylmethanofuran:tetrahydromethanopterin N-formyltransferase (EC: 2.3.1.101), methenyltetrahydromethanopterin cyclohydrolase (EC: 3.5.4.27) methylenetetrahydromethanopterin dehydrogenase (EC: 1.5.98.1), and 5,10-methylenetetrahydromethanopterin reductase (EC: 1.5.98.2) . This result was in accordance with the promotion of hydrogenotrophic methanogens (*Methanobacterium* and *Methanothermobacter*, etc.) and formation of their substrates (H_2/CO_2) under ON-SSBC addition (Fig. S4, Fig. 6B). The enhancement of hydrogenotrophic pathways might be contributed from the combined effect of SSBC and the released oxygen NBs, which are reported to have promotional effects on hydrogenotrophic methanogens (Wang et al., 2020d; Yang et al., 2020).

For acetoclastic methanogenesis, acetate is firstly converted to acetyl-CoA through two potential pathways, the low-affinity acetate kinase (ackA)-phosphotransacetylase (PTA) system (EC:2.3.1.8 and EC:2.3.1.8) utilized by *Methanosarcins* and the high-affinity adenosine monophosphate (AMP)-forming acetyl-CoA synthetase (EC: 6.2.1.1) utilized by *Methanosaeta.*

Then acetyl-CoA is converted to the precursor of methane (5-MethylTHMPT) by acetyl-CoA decarbonylase/synthase (EC: 2.3.1.169) (Duan et al., 2021; Zhao et al., 2020). It is worth noting that the module (M00357) related to acetoclastic pathway was enriched by SSBC, however, its abundance was reduced by ON-SSBC. Similar results could be observed in the abundances of related genes that encode the aforementioned enzymes. The gaps between SSBC and ON-SSBC narrowed on day 16, and the abundance of *ackA* of SSBC even passed SSBC. Similarly, there are researchers claim that the supplementation of NBW enhanced the activity of acetoclastic methanogens (Fan et al., 2021; Wang et al., 2020d). To summarize, the enhancement of methane production by SSBC addition mainly derived from promotion of acetoclastic pathway, while the other two methanogenic pathways including methylotrophic and hydrogenotrophic pathways were also promoted by ON-SSBC addition.

Furthermore, the abundance of genes for enzyme F420 (EC: 1.12.98.1), an essential coenzyme for methanogenesis in the AD process, were also enhanced with the addition of ON-SSBC (Fig. 6B), which indicated that the increase of the activity of methanogens (Fan et al., 2020). Similar results were reported by other researchers that the activity of coenzyme F420 was enhanced with addition of Air-NB or O_2-NB (Hou et al., 2021a; Hou et al., 2021b) and biochar (Lü et al., 2020; Wang et al., 2020a). Interestingly, less genes associated with formation of pili and cytochrome (e. g. *PilA* and *OmcS*) that serve as electron transfer agent of DIET was detected with ON-SSBC addition compared with CK or SSBC. Nevertheless, the electron accepting methanogens (*Methanothrix* and *Methanosarcina*) in DIET pathway were enriched by ON-SSBC as discussed above (Fig. S4). It might be because that the enhanced conductibility by biochar and nanobubbles in AD systems of ON-SSBC group acted as substitute for e-pili or c-type cytochromes and accelerated methane production (Park et al., 2018; Qi et al., 2021; Wang et al., 2020d; Zhao et al., 2020).. Similar results were reported by other researchers that conductive materials could act as conduit to save energy for growth rather than developing conductive pili or cytochrome for the electron transfer and therefore benefit methanogenesis (Park et al., 2018; Wang and Lee, 2021). It should be mentioned that these speculations were based on metagenomics (DNA level), rather than metatranscriptomics or metaproteomics (RNA or protein level), which are required to further explore the active functions involved in the DIET pathway in future study.

4. Conclusions

The enhancement and underlying mechanisms on biogas production by addition of oxygen nanobubble-loaded biochar (ON-SSBC) before AD of WAS were investigated in this study. The following conclusions were drawn.

- Sewage sludge biochar (SSBC) was produced to be a porous material with larger surface area and presented a good condition for nanobubbles loading (18.42 ± 0.96 mg oxygen per gram SSBC);
- Nanobubbles with a mean diameter of 152 nm can be efficiently released from ON-SSBC and the concentration could reach 8.97×10^7 particles/mL in water solution with 1% (w/v) addition;
- Addition of ON-SSBC substantially increased methane production by 4.86 and 3.14 times compared to group with no additives addition (CK) and group with sewage sludge biochar (SSBC) addition only
- The underlying mechanisms of enhanced biogas production under ON-SSBC addition are 1) promotion of sludge cells disruption and EPS hydrolysis; 2) enrichment of hydrolytic bacteria (*Firmicutes* and *Bacteroidetes*) and genes for hydrolases (glycosidases and peptidases) by microaerobic conditions attribute to oxygen nanobubbles released from ON-SSBC; 3) enhancement of genes related to SCFAs generation and consumption; 4) enrichment of acetoclastic, methylotrophic and hydrogenotrophic pathway and related methanogens (*Methanosarcinales*, *Methanosphaera*, and Methanobacterium; 5) increase of genes responsible for enzyme F420 biosynthesis and enhancement of DIET.

Acknowledgments

This work was supported by Jing-Jin-Ji Regional Integrated Environmental Improvement-National Science and Technology Major Project (2026ZD1213900 and 2025ZD1204700), and National Natural Science Foundation of China (42230411, 42407161 and 52500064).

Author Contributions

C.J. conceived and designed the research and wrote the manuscript. D.W, H.W., and X.W., performed the experiments. X. W. and X. Z. supervised the project. All authors have read the final manuscript and approved it.

628 **Reference**

629 Agarwal, A., Ng, W.J. and Liu, Y. 2011. Principle and applications of microbubble and nanobubble
630 technology for water treatment. Chemosphere 84(9), 1175-1180.
631 Amani, T., Nosrati, M. and Sreekrishnan, T.R. 2010. Anaerobic digestion from the viewpoint of
632 microbiological, chemical, and operational aspects — a review. Environmental Reviews
633 18(NA), 255-278.
634 Beraud-Martinez, L.K., Gomez-Gil, B., Franco-Nava, M.A., Almazan-Rueda, P. and Betancourt-
635 Lozano, M. 2021. A metagenomic assessment of microbial communities in anaerobic
636 bioreactors and sediments: Taxonomic and functional relationships. Anaerobe 68, 102296.
637 Brenner, M.P. and Lohse, D. 2008. Dynamic equilibrium mechanism for surface nanobubble
638 stabilization. Phys Rev Lett 101(21), 214505.
639 Campanaro, S., Treu, L., Kougias, P.G., Luo, G. and Angelidaki, I. 2018. Metagenomic binning
640 reveals the functional roles of core abundant microorganisms in twelve full-scale biogas
641 plants. Water Res 140, 123-134.
642 Carabeo-Pérez, A., Guerra-Rivera, G., Ramos-Leal, M. and Jiménez-Hernández, J. 2019.
643 Metagenomic approaches: effective tools for monitoring the structure and functionality of
644 microbiomes in anaerobic digestion systems. Applied Microbiology and Biotechnology
645 103(23-24), 9379-9390.
646 Chen, S., Rotaru, A.E., Shrestha, P.M., Malvankar, N.S., Liu, F., Fan, W., Nevin, K.P. and Lovley, D.R.
647 2014. Promoting interspecies electron transfer with biochar. Sci Rep 4, 5019.
648 Chen, Y., Yang, Z., Zhang, Y., Xiang, Y., Xu, R., Jia, M., Cao, J. and Xiong, W. 2020. Effects of
649 different conductive nanomaterials on anaerobic digestion process and microbial community
650 of sludge. Bioresour Technol 304, 123016.
651 Choi, J.M., Han, S.K. and Lee, C.Y. 2018. Enhancement of methane production in anaerobic digestion
652 of sewage sludge by thermal hydrolysis pretreatment. Bioresour Technol 259, 207-213.
653 Chuenchart, W., Karki, R., Shitanaka, T., Marcelino, K.R., Lu, H. and Khanal, S.K. 2021. Nanobubble
654 technology in anaerobic digestion: A review. Bioresour Technol 329, 124916.
655 Cooney, M.J., Lewis, K., Harris, K., Zhang, Q. and Yan, T. 2016. Start up performance of biochar
656 packed bed anaerobic digesters. Journal of Water Process Engineering 9, e7-e13.
657 Ding, H.H., Chang, S. and Liu, Y. 2017. Biological hydrolysis pretreatment on secondary sludge:

Enhancement of anaerobic digestion and mechanism study. Bioresour Technol 244(Pt 1), 989-995.

Duan, X., Chen, Y., Feng, L. and Zhou, Q. 2021. Metagenomic analysis reveals nonylphenol-shaped acidification and methanogenesis during sludge anaerobic digestion. Water Res 196, 117004.

Ebina, K., Shi, K., Hirao, M., Hashimoto, J., Kawato, Y., Kaneshiro, S., Morimoto, T., Koizumi, K. and Yoshikawa, H. 2013. Oxygen and air nanobubble water solution promote the growth of plants, fishes, and mice. PLoS One 8(6), e65339.

Fagbohungbe, M.O., Herbert, B.M., Hurst, L., Ibeto, C.N., Li, H., Usmani, S.Q. and Semple, K.T. 2017. The challenges of anaerobic digestion and the role of biochar in optimizing anaerobic digestion. Waste Manag 61, 236-249.

Fan, Y., Lei, Z., Guo, Z., Huang, W., Wang, D., Wang, X., Zhang, Z. and Shimizu, K. 2020. Enhanced solubilization of solid organics and methane production by anaerobic digestion of swine manure under nano-bubble water addition. Bioresour Technol 299, 122512.

Fan, Y., Yang, X., Lei, Z., Zhang, Z., Kobayashi, M., Adachi, Y. and Shimizu, K. 2021. Alleviation of ammonia inhibition via nano-bubble water supplementation during anaerobic digestion of ammonia-rich swine manure: Buffering capacity promotion and methane production enhancement. Bioresour Technol 333, 125131.

Felden, J., Wenzhöfer, F., Feseker, T. and Boetius, A. 2010. Transport and consumption of oxygen and methane in different habitats of the Håkon Mosby Mud Volcano (HMMV). Limnology and Oceanography 55(6), 2366-2380.

Figueiredo, C., Lopes, H., Coser, T., Vale, A., Busato, J., Aguiar, N., Novotny, E. and Canellas, L. 2017. Influence of pyrolysis temperature on chemical and physical properties of biochar from sewage sludge. Archives of Agronomy and Soil Science 64(6), 881-889.

Fu, S.-F., Wang, F., Shi, X.-S. and Guo, R.-B. 2016. Impacts of microaeration on the anaerobic digestion of corn straw and the microbial community structure. Chemical Engineering Journal 287, 523-528.

Gantzer, P.A., Bryant, L.D. and Little, J.C. 2009. Effect of hypolimnetic oxygenation on oxygen depletion rates in two water-supply reservoirs. Water Res 43(6), 1700-1710.

Guo, B., Yu, N., Weissbrodt, D.G. and Liu, Y. 2021. Effects of micro-aeration on microbial niches and antimicrobial resistances in blackwater anaerobic digesters. Water Res 196, 117035.

688 Guo, Z., Ma, L., Dai, Q., Ao, R., Liu, H., Wei, Y. and Mu, L. 2020. Role of extracellular polymeric
689 substances in sludge dewatering under modified corn-core powder and sludge-based biochar
690 pretreatments. Ecotoxicol Environ Saf 202, 110882.
691 Hao, X., Chen, Q., van Loosdrecht, M.C.M., Li, J. and Jiang, H. 2020. Sustainable disposal of excess
692 sludge: Incineration without anaerobic digestion. Water Res 170, 115298.
693 Haris, S., Qiu, X., Klammler, H. and Mohamed, M.M.A. 2020. The use of micro-nano bubbles in
694 groundwater remediation: A comprehensive review. Groundwater for Sustainable
695 Development 11.
696 Hou, T., Zhao, J., Lei, Z., Shimizu, K. and Zhang, Z. 2021a. Addition of air-nanobubble water to
697 mitigate the inhibition of high salinity on co-production of hydrogen and methane from two-
698 stage anaerobic digestion of food waste. Journal of Cleaner Production 314.
699 Hou, T., Zhao, J., Lei, Z., Shimizu, K. and Zhang, Z. 2021b. Enhanced energy recovery via separate
700 hydrogen and methane production from two-stage anaerobic digestion of food waste with
701 nanobubble water supplementation. Sci Total Environ 761, 143234.
702 Kavitha, S., Jayashree, C., Adish Kumar, S., Yeom, I.T. and Rajesh Banu, J. 2014. The enhancement
703 of anaerobic biodegradability of waste activated sludge by surfactant mediated biological
704 pretreatment. Bioresour Technol 168, 159-166.
705 Khalid, Z.B., Siddique, M.N.I., Nayeem, A., Adyel, T.M., Ismail, S.B. and Ibrahim, M.Z. 2021.
706 Biochar application as sustainable precursors for enhanced anaerobic digestion: A systematic
707 review. Journal of Environmental Chemical Engineering 9(4).
708 Khanh Nguyen, V., Kumar Chaudhary, D., Hari Dahal, R., Hoang Trinh, N., Kim, J., Chang, S.W.,
709 Hong, Y., Duc La, D., Nguyen, X.C., Hao Ngo, H., Chung, W.J. and Nguyen, D.D. 2021.
710 Review on pretreatment techniques to improve anaerobic digestion of sewage sludge. Fuel
711 285.
712 Kor-Bicakci, G. and Eskicioglu, C. 2019. Recent developments on thermal municipal sludge
713 pretreatment technologies for enhanced anaerobic digestion. Renewable and Sustainable
714 Energy Reviews 110, 423-443.
715 Kumar, M., Dutta, S., You, S., Luo, G., Zhang, S., Show, P.L., Sawarkar, A.D., Singh, L. and Tsang,
716 D.C.W. 2021. A critical review on biochar for enhancing biogas production from anaerobic
717 digestion of food waste and sludge. Journal of Cleaner Production 305.

718 Li, Y., Chen, Y. and Wu, J. 2019. Enhancement of methane production in anaerobic digestion process:
719 A review. Applied Energy 240, 120-137.
720 Lim, E.Y., Tian, H., Chen, Y., Ni, K., Zhang, J. and Tong, Y.W. 2020. Methanogenic pathway and
721 microbial succession during start-up and stabilization of thermophilic food waste anaerobic
722 digestion with biochar. Bioresour Technol 314, 123751.
723 Liu, C.G., Xue, C., Lin, Y.H. and Bai, F.W. 2013. Redox potential control and applications in
724 microaerobic and anaerobic fermentations. Biotechnol Adv 31(2), 257-265.
725 Liu, H. and Fang, H.H.P. 2002. Extraction of extracellular polymeric substances (EPS) of sludges.
726 Journal of Biotechnology 95(3), 249-256.
727 Liu, X., Wu, Y., Xu, Q., Du, M., Wang, D., Yang, Q., Yang, G., Chen, H., Zeng, T., Liu, Y., Wang, Q.
728 and Ni, B.-J. 2021. Mechanistic insights into the effect of poly ferric sulfate on anaerobic
729 digestion of waste activated sludge. Water Research 189, 116645.
730 Liu, Z., Zhou, A., Liu, H., Wang, S., Liu, W., Wang, A. and Yue, X. 2020. Extracellular polymeric
731 substance decomposition linked to hydrogen recovery from waste activated sludge: Role of
732 peracetic acid and free nitrous acid co-pretreatment in a prefermentation-bioelectrolysis
733 cascading system. Water Res 176, 115724.
734 Lohse, D. and Zhang, X. 2015. Surface nanobubbles and nanodroplets. Reviews of Modern Physics
735 87(3), 981-1035.
736 Lou, S.-T., Ouyang, Z.-Q., Zhang, Y., Li, X.-J., Hu, J., Li, M.-Q. and Yang, F.-J. 2000. Nanobubbles
737 on solid surface imaged by atomic force microscopy. Journal of Vacuum Science &
738 Technology B: Microelectronics and Nanometer Structures 18(5).
739 Lü, C., Shen, Y., Li, C., Zhu, N. and Yuan, H. 2020. Redox-Active Biochar and Conductive Graphite
740 Stimulate Methanogenic Metabolism in Anaerobic Digestion of Waste-Activated Sludge:
741 Beyond Direct Interspecies Electron Transfer. ACS Sustainable Chemistry & Engineering
742 8(33), 12626-12636.
743 Lu, F., Bize, A., Guillot, A., Monnet, V., Madigou, C., Chapleur, O., Mazeas, L., He, P. and Bouchez, T.
744 2014. Metaproteomics of cellulose methanisation under thermophilic conditions reveals a
745 surprisingly high proteolytic activity. ISME J 8(1), 88-102.
746 Lu, H., Zhang, W., Wang, S., Zhuang, L., Yang, Y. and Qiu, R. 2013. Characterization of sewage
747 sludge-derived biochars from different feedstocks and pyrolysis temperatures. Journal of

748 Analytical and Applied Pyrolysis 102, 137-143.
749 Luo, C., Lu, F., Shao, L. and He, P. 2015. Application of eco-compatible biochar in anaerobic
750 digestion to relieve acid stress and promote the selective colonization of functional microbes.
751 Water Res 68, 710-718.
752 Ma, K., Wang, W., Liu, Y., Bao, L., Cui, Y., Kang, W., Wu, Q. and Xin, X. 2021. Insight into the
753 performance and microbial community profiles of magnetite-amended anaerobic digestion:
754 Varying promotion effects at increased loads. Bioresour Technol 329, 124928.
755 Narihiro, T., Nobu, M.K., Kim, N.-K., Kamagata, Y. and Liu, W.-T. 2015. The nexus of syntrophy-
756 associated microbiota in anaerobic digestion revealed by long-term enrichment and
757 community survey. Environmental Microbiology 17(5), 1707-1720.
758 Narihiro, T. and Sekiguchi, Y. 2007. Microbial communities in anaerobic digestion processes for
759 waste and wastewater treatment: a microbiological update. Curr Opin Biotechnol 18(3), 273-
760 278.
761 Nguyen, D. and Khanal, S.K. 2018. A little breath of fresh air into an anaerobic system: How
762 microaeration facilitates anaerobic digestion process. Biotechnol Adv 36(7), 1971-1983.
763 Nguyen, D., Wu, Z., Shrestha, S., Lee, P.H., Raskin, L. and Khanal, S.K. 2019. Intermittent micro-
764 aeration: New strategy to control volatile fatty acid accumulation in high organic loading
765 anaerobic digestion. Water Res 166, 115080.
766 Ohgaki, K., Khanh, N.Q., Joden, Y., Tsuji, A. and Nakagawa, T. 2010. Physicochemical approach to
767 nanobubble solutions. Chemical Engineering Science 65(3), 1296-1300.
768 Pan, J., Ma, J., Zhai, L., Luo, T., Mei, Z. and Liu, H. 2019. Achievements of biochar application for
769 enhanced anaerobic digestion: A review. Bioresour Technol 292, 122058.
770 Park, J.H., Park, J.H., Je Seong, H., Sul, W.J., Jin, K.H. and Park, H.D. 2018. Metagenomic insight
771 into methanogenic reactors promoting direct interspecies electron transfer via granular
772 activated carbon. Bioresour Technol 259, 414-422.
773 Qi, Q., Sun, C., Zhang, J., He, Y. and Wah Tong, Y. 2021. Internal enhancement mechanism of biochar
774 with graphene structure in anaerobic digestion: The bioavailability of trace elements and
775 potential direct interspecies electron transfer. Chemical Engineering Journal 406.
776 Rotaru, A.-E., Shrestha, P.M., Liu, F., Shrestha, M., Shrestha, D., Embree, M., Zengler, K., Wardman,
777 C., Nevin, K.P. and Lovley, D.R. 2014. A new model for electron flow during anaerobic

778 digestion: direct interspecies electron transfer to Methanosaeta for the reduction of carbon
779 dioxide to methane. Energy Environ. Sci. 7(1), 408-415.
780 Ruan, D., Zhou, Z., Pang, H., Yao, J., Chen, G. and Qiu, Z. 2019. Enhancing methane production of
781 anaerobic sludge digestion by microaeration: Enzyme activity stimulation, semi-continuous
782 reactor validation and microbial community analysis. Bioresour Technol 289, 121643.
783 Shen, Y., Yu, Y., Zhang, Y., Urgun-Demirtas, M., Yuan, H., Zhu, N. and Dai, X. 2021. Role of redox-
784 active biochar with distinctive electrochemical properties to promote methane production in
785 anaerobic digestion of waste activated sludge. Journal of Cleaner Production 278.
786 Shi, W., Pan, G., Chen, Q., Song, L., Zhu, L. and Ji, X. 2018. Hypoxia Remediation and Methane
787 Emission Manipulation Using Surface Oxygen Nanobubbles. Environ Sci Technol 52(15),
788 8712-8717.
789 Singh, S., Kumar, V., Dhanjal, D.S., Datta, S., Bhatia, D., Dhiman, J., Samuel, J., Prasad, R. and Singh,
790 J. 2020. A sustainable paradigm of sewage sludge biochar: Valorization, opportunities,
791 challenges and future prospects. Journal of Cleaner Production 269.
792 Tan, B.H., An, H. and Ohl, C.D. 2020. How Bulk Nanobubbles Might Survive. Phys Rev Lett
793 124(13), 134503.
794 Tang, Y., Alam, M.S., Konhauser, K.O., Alessi, D.S., Xu, S., Tian, W. and Liu, Y. 2019. Influence of
795 pyrolysis temperature on production of digested sludge biochar and its application for
796 ammonium removal from municipal wastewater. Journal of Cleaner Production 209, 927-936.
797 Temesgen, T., Bui, T.T., Han, M., Kim, T.I. and Park, H. 2017. Micro and nanobubble technologies as
798 a new horizon for water-treatment techniques: A review. Adv Colloid Interface Sci 246, 40-51.
799 Tian, T., Qiao, S., Li, X., Zhang, M. and Zhou, J. 2017. Nano-graphene induced positive effects on
800 methanogenesis in anaerobic digestion. Bioresour Technol 224, 41-47.
801 Treu, L., Tsapekos, P., Peprah, M., Campanaro, S., Giacomini, A., Corich, V., Kougias, P.G. and
802 Angelidaki, I. 2019. Microbial profiling during anaerobic digestion of cheese whey in
803 reactors operated at different conditions. Bioresour Technol 275, 375-385.
804 Ulatowski, K. and Sobieszuk, P. 2020. Gas nanobubble dispersions as the important agent in
805 environmental processes – generation methods review. Water and Environment Journal
806 34(S1), 772-790.
807 Wang, C., Liu, Y., Gao, X., Chen, H., Xu, X. and Zhu, L. 2018a. Role of biochar in the granulation of

anaerobic sludge and improvement of electron transfer characteristics. Bioresour Technol 268, 28-35.

Wang, D., Yang, X., Tian, C., Lei, Z., Kobayashi, N., Kobayashi, M., Adachi, Y., Shimizu, K. and Zhang, Z. 2019a. Characteristics of ultra-fine bubble water and its trials on enhanced methane production from waste activated sludge. Bioresour Technol 273, 63-69.

Wang, G., Li, Y., Sheng, L., Xing, Y., Liu, G., Yao, G., Ngo, H.H., Li, Q., Wang, X.C., Li, Y.Y. and Chen, R. 2020a. A review on facilitating bio-wastes degradation and energy recovery efficiencies in anaerobic digestion systems with biochar amendment. Bioresour Technol 314, 123777.

Wang, L., Miao, X., Ali, J., Lyu, T. and Pan, G. 2018b. Quantification of Oxygen Nanobubbles in Particulate Matters and Potential Applications in Remediation of Anaerobic Environment. ACS Omega 3(9), 10624-10630.

Wang, P., Peng, H., Adhikari, S., Higgins, B., Roy, P., Dai, W. and Shi, X. 2020b. Enhancement of biogas production from wastewater sludge via anaerobic digestion assisted with biochar amendment. Bioresour Technol 309, 123368.

Wang, W. and Lee, D.J. 2021. Direct interspecies electron transfer mechanism in enhanced methanogenesis: A mini-review. Bioresour Technol 330, 124980.

Wang, X., Daigger, G., de Vries, W., Kroeze, C., Yang, M., Ren, N.Q., Liu, J. and Butler, D. 2019b. Impact hotspots of reduced nutrient discharge shift across the globe with population and dietary changes. Nat Commun 10(1), 2627.

Wang, X., Lei, Z., Shimizu, K., Zhang, Z. and Lee, D.-J. 2021. Recent advancements in nanobubble water technology and its application in energy recovery from organic solid wastes towards a greater environmental friendliness of anaerobic digestion system. Renewable and Sustainable Energy Reviews 145.

Wang, X., Yuan, T., Guo, Z., Han, H., Lei, Z., Shimizu, K., Zhang, Z. and Lee, D.J. 2020c. Enhanced hydrolysis and acidification of cellulose at high loading for methane production via anaerobic digestion supplemented with high mobility nanobubble water. Bioresour Technol 297, 122499.

Wang, X., Yuan, T., Lei, Z., Kobayashi, M., Adachi, Y., Shimizu, K., Lee, D.-J. and Zhang, Z. 2020d. Supplementation of O2-containing gas nanobubble water to enhance methane production from anaerobic digestion of cellulose. Chemical Engineering Journal 398.

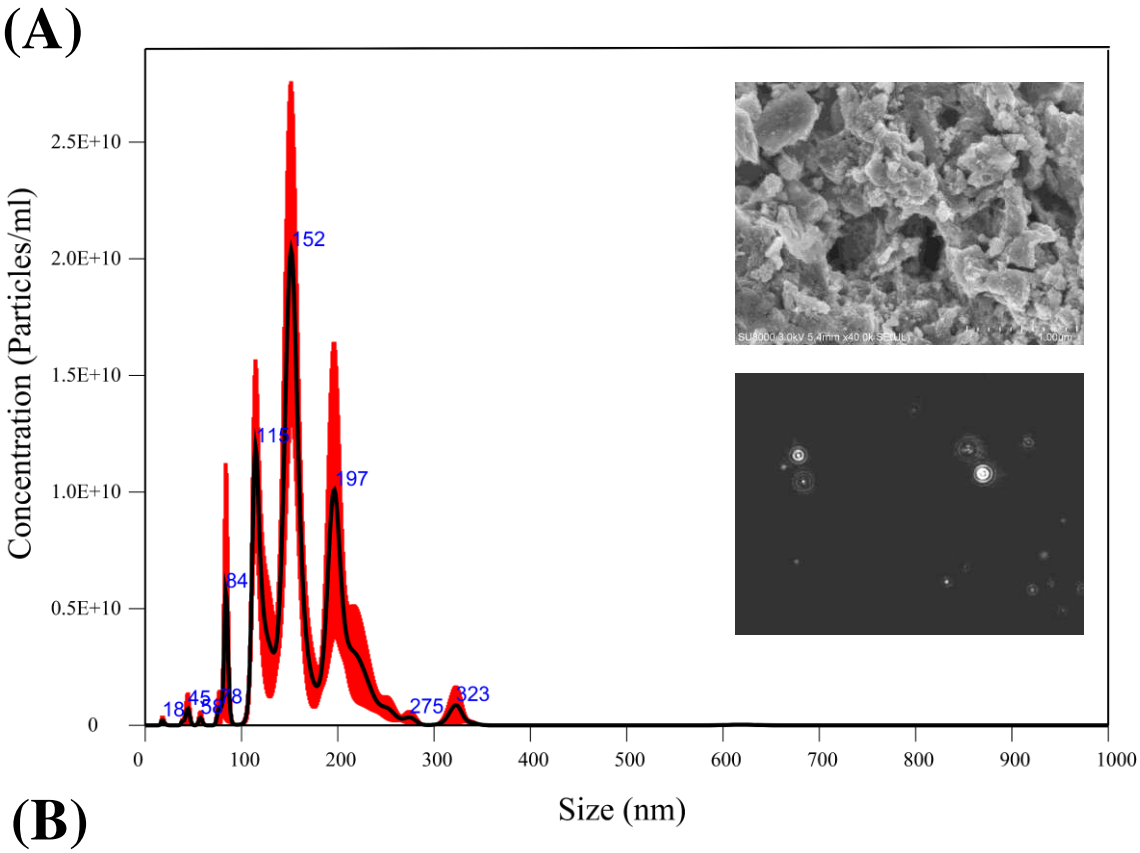
838 Wei, J., Hao, X., van Loosdrecht, M.C.M. and Li, J. 2018. Feasibility analysis of anaerobic digestion
839 of excess sludge enhanced by iron: A review. Renewable and Sustainable Energy Reviews 89,
840 16-26.
841 Weijs, J.H. and Lohse, D. 2013. Why surface nanobubbles live for hours. Phys Rev Lett 110(5),
842 054501.
843 Wu, B., Yang, Q., Yao, F., Chen, S., He, L., Hou, K., Pi, Z., Yin, H., Fu, J., Wang, D. and Li, X. 2019.
844 Evaluating the effect of biochar on mesophilic anaerobic digestion of waste activated sludge
845 and microbial diversity. Bioresour Technol 294, 122235.
846 Wu, X., Li, X., Yang, Q., Xu, Q., Tao, Z., Huang, X., Wu, Y., Tao, L., Pi, Z., Chen, Z. and Wang, D.
847 2020a. Effect of citric acid on extracellular polymeric substances disruption and cell lysis in
848 the waste activated sludge by pH regulation. Bioresour Technol 302, 122859.
849 Wu, Y., Wang, S., Liang, D. and Li, N. 2020b. Conductive materials in anaerobic digestion: From
850 mechanism to application. Bioresour Technol 298, 122403.
851 Xiao, K., Abbt-Braun, G. and Horn, H. 2020. Changes in the characteristics of dissolved organic
852 matter during sludge treatment: A critical review. Water Res 187, 116441.
853 Xie, J., Zhu, X., Liao, Q., Wang, H. and Ding, Y.-D. 2012. Dynamics of bubble formation and
854 detachment from an immersed micro-orifice on a plate. International Journal of Heat and
855 Mass Transfer 55(11-12), 3205-3213.
856 Xing, B.-S. and Wang, X.C. 2021. High-rate mesophilic co-digestion with food waste and waste
857 activated sludge through a low-magnitude increasing loading regime: Performance and
858 microorganism characteristics. Science of The Total Environment 777.
859 Xu, Q., Huang, Q.-S., Wei, W., Sun, J., Dai, X. and Ni, B.-J. 2020a. Improving the treatment of waste
860 activated sludge using calcium peroxide. Water Research 187.
861 Xu, W., Fu, S., Yang, Z., Lu, J. and Guo, R. 2018. Improved methane production from corn straw by
862 microaerobic pretreatment with a pure bacteria system. Bioresour Technol 259, 18-23.
863 Xu, Y., Lu, Y., Zheng, L., Wang, Z. and Dai, X. 2020b. Perspective on enhancing the anaerobic
864 digestion of waste activated sludge. J Hazard Mater 389, 121847.
865 Yan, P., Zhao, Y., Zhang, H., Chen, S., Zhu, W., Yuan, X. and Cui, Z. 2020. A comparison and
866 evaluation of the effects of biochar on the anaerobic digestion of excess and anaerobic sludge.
867 Sci Total Environ 736, 139159.

868 Yang, H.-J., Yang, Z.-M., Xu, X.-H. and Guo, R.-B. 2020. Increasing the methane production rate of
869 hydrogenotrophic methanogens using biochar as a biocarrier. Bioresource Technology 302.
870 Yang, X., Nie, J., Wang, D., Zhao, Z., Kobayashi, M., Adachi, Y., Shimizu, K., Lei, Z. and Zhang, Z.
871 2019. Enhanced hydrolysis of waste activated sludge for methane production via anaerobic
872 digestion under N2-nanobubble water addition. Sci Total Environ 693, 133524.
873 Yu, G.H., He, P.J., Shao, L.M. and Zhu, Y.S. 2008. Extracellular proteins, polysaccharides and
874 enzymes impact on sludge aerobic digestion after ultrasonic pretreatment. Water Res 42(8-9),
875 1925-1934.
876 Zhang, H., Lyu, T., Bi, L., Tempero, G., Hamilton, D.P. and Pan, G. 2018a. Combating
877 hypoxia/anoxia at sediment-water interfaces: A preliminary study of oxygen nanobubble
878 modified clay materials. Sci Total Environ 637-638, 550-560.
879 Zhang, L., Gong, X., Wang, L., Guo, K., Cao, S. and Zhou, Y. 2021. Metagenomic insights into the
880 effect of thermal hydrolysis pre-treatment on microbial community of an anaerobic digestion
881 system. Sci Total Environ 791, 148096.
882 Zhang, L., Li, F., Kuroki, A., Loh, K.C., Wang, C.H., Dai, Y. and Tong, Y.W. 2020. Methane yield
883 enhancement of mesophilic and thermophilic anaerobic co-digestion of algal biomass and
884 food waste using algal biochar: Semi-continuous operation and microbial community analysis.
885 Bioresour Technol 302, 122892.
886 Zhang, M., Li, J. and Wang, Y. 2019a. Impact of biochar-supported zerovalent iron nanocomposite on
887 the anaerobic digestion of sewage sludge. Environmental Science and Pollution Research
888 26(10), 10292-10305.
889 Zhang, M., Li, J., Wang, Y. and Yang, C. 2019b. Impacts of different biochar types on the anaerobic
890 digestion of sewage sludge. RSC Advances 9(72), 42375-42386.
891 Zhang, P., Zheng, S., Liu, J., Wang, B., Liu, F. and Feng, Y. 2018b. Surface properties of activated
892 sludge-derived biochar determine the facilitating effects on Geobacter co-cultures. Water Res
893 142, 441-451.
894 Zhao, W., Yang, H., He, S., Zhao, Q. and Wei, L. 2021. A review of biochar in anaerobic digestion to
895 improve biogas production: Performances, mechanisms and economic assessments. Bioresour
896 Technol 341, 125797.
897 Zhao, Z., Wang, J., Li, Y., Zhu, T., Yu, Q., Wang, T., Liang, S. and Zhang, Y. 2020. Why do DIETers

like drinking: Metagenomic analysis for methane and energy metabolism during anaerobic digestion with ethanol. Water Res 171, 115425.

Zhen, G., Lu, X., Kato, H., Zhao, Y. and Li, Y.-Y. 2017. Overview of pretreatment strategies for enhancing sewage sludge disintegration and subsequent anaerobic digestion: Current advances, full-scale application and future perspectives. Renewable and Sustainable Energy Reviews 69, 559-577.

Zhou, H., Brown, R.C. and Wen, Z. 2020. Biochar as an Additive in Anaerobic Digestion of Municipal Sludge: Biochar Properties and Their Effects on the Digestion Performance. ACS Sustainable Chemistry & Engineering 8(16), 6391-6401.



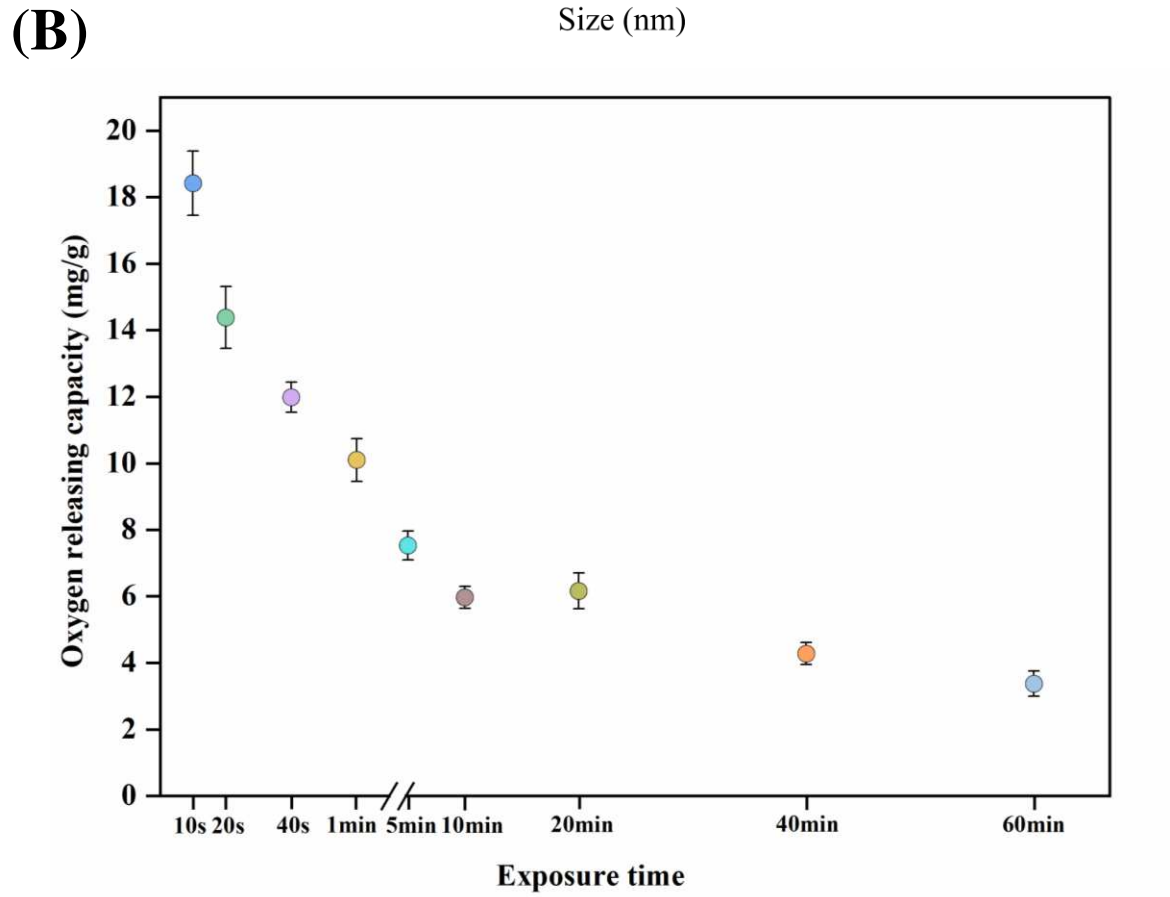


Fig. 1. Nanobubble concentrations and size distribution in water solution with 1% (w/v) ON-SSBC addition, SEM picture of produced SSBC (above) and sample video frame of nanobubbles released from ON-SSBC (below) (A) and effect of air exposure time on oxygen releasing capacity of ON-SSBC (B).

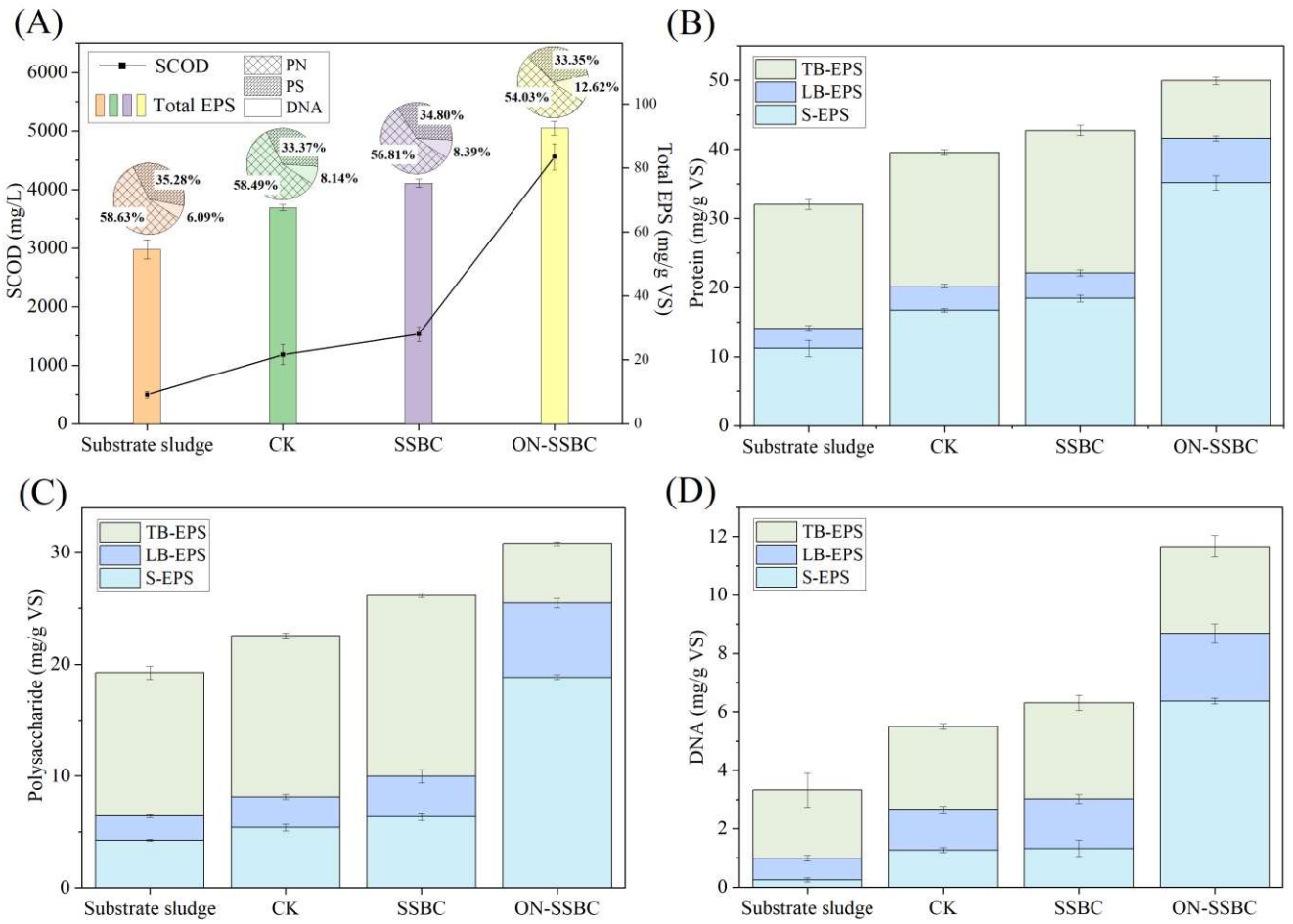


Fig. 2. Effects of ON-SSBC addition on SCOD release and EPS distribution and migration

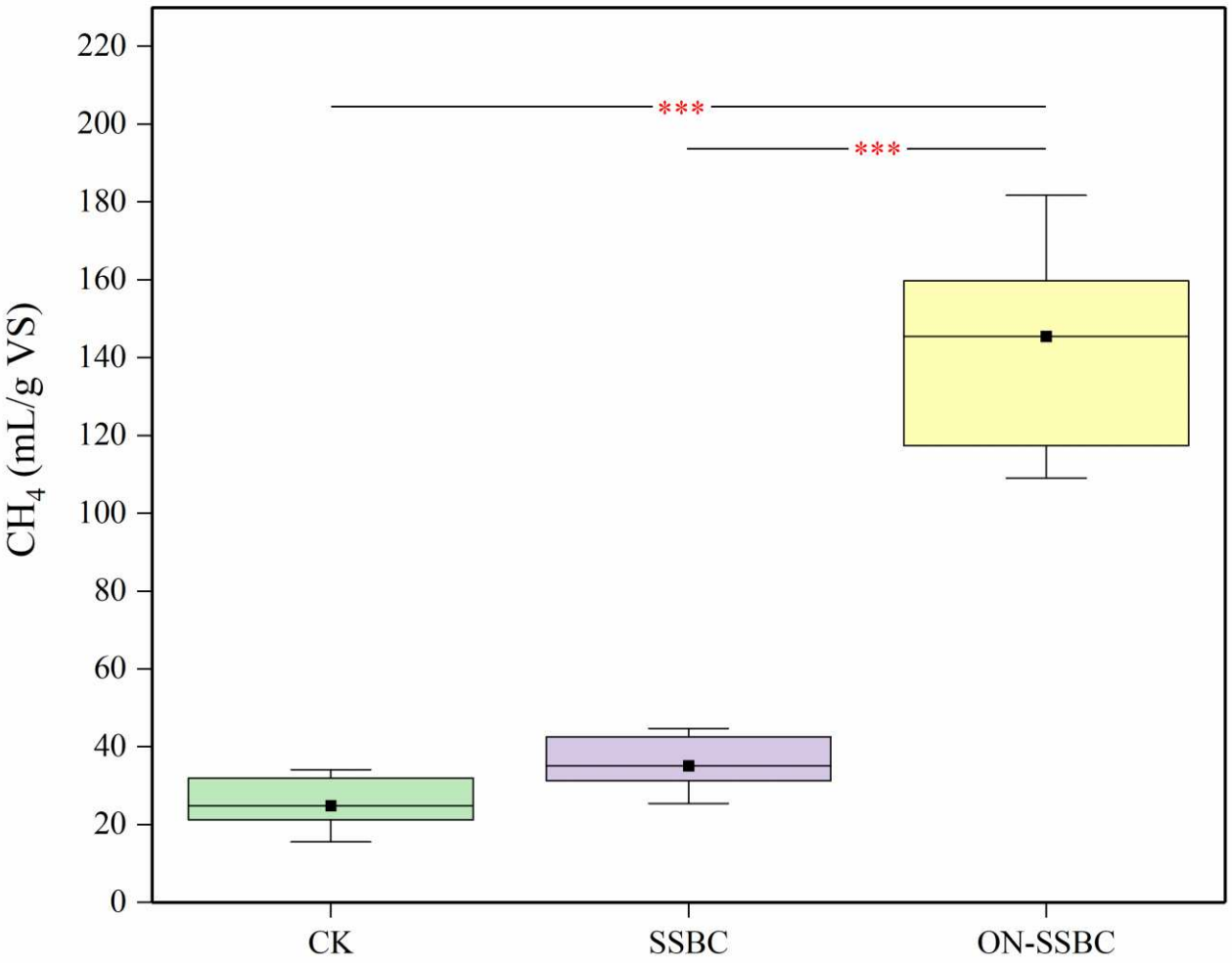


Fig. 3. Total methane production during anaerobic digestion in different groups.

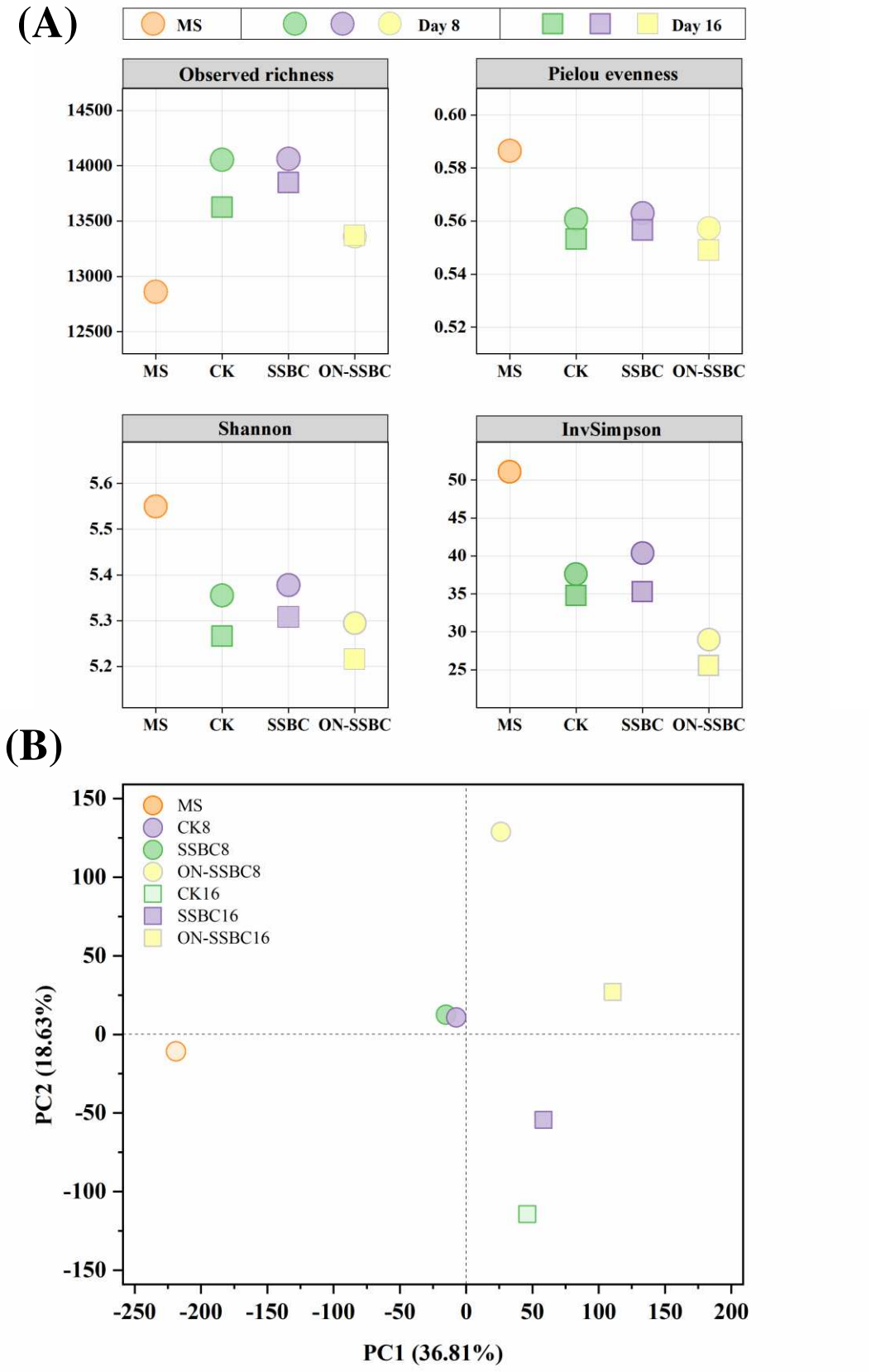


Fig. 4. Alpha diversities of microbial communities (A) and principal component analysis (PCA) of the whole microbial community on species level (B) of sludge samples from different groups



Fig. 5. The heatmap showing the top 100 bacterial species in each sample. The green triangle and pentagram represented the significant decrease of corresponding species in ON-SSBC compared with SSBC on day 8 and day 16,respectively. . The red triangle and pentagram represented the significant increase of corresponding species in ON-SSBC compared with SSBC on day 8 and day 16,respectively. (Chi-square test, $P < 0.001$)

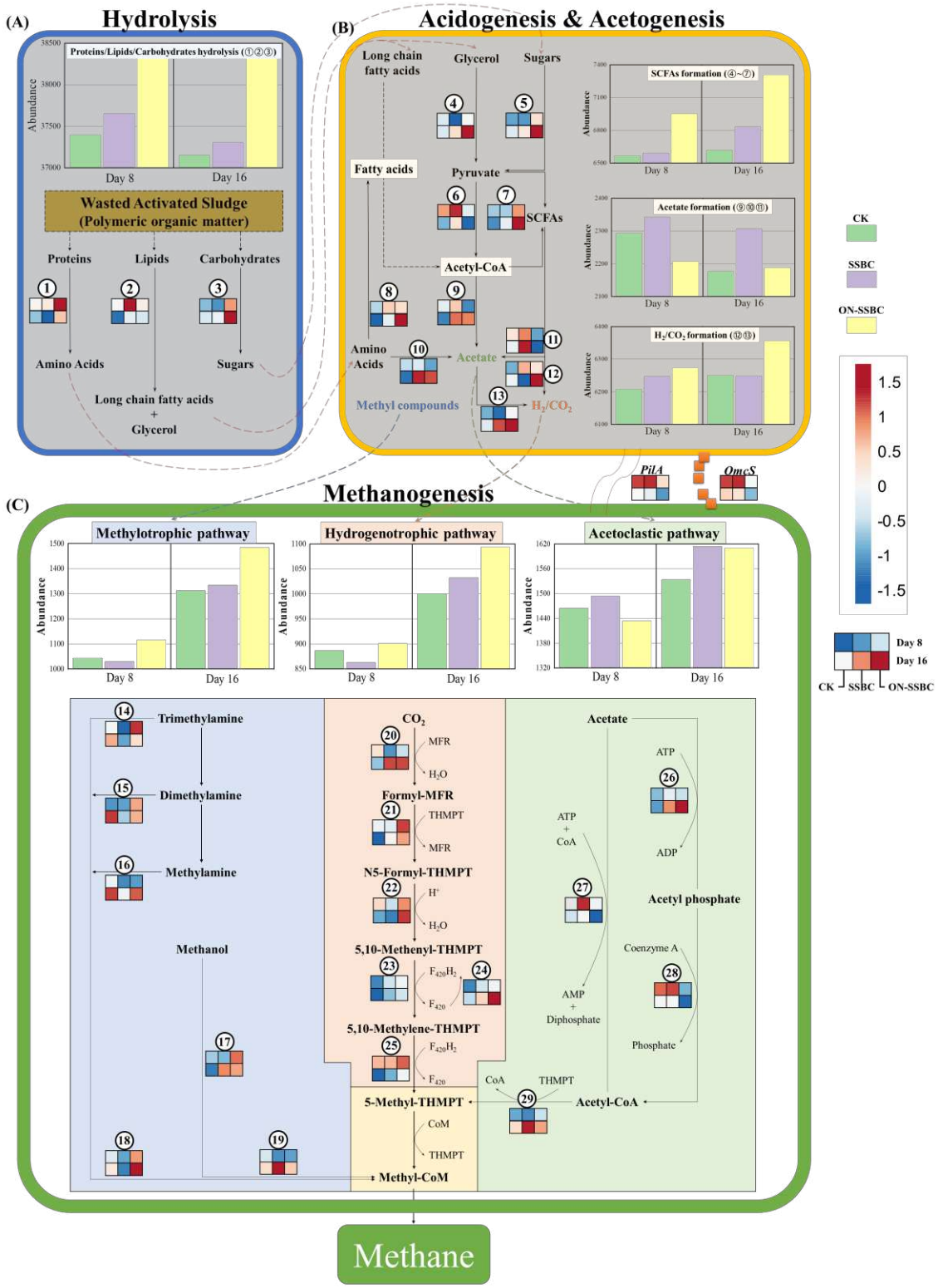


Fig. 6. Metabolic pathways related to hydrolysis (A), acidogenesis & Acetogenesis (B), and methanogenesis (C). 1~29 represented the reaction of corresponding pathways and abundance information of related enzymes (heatmap); bar chart represented the total abundance of enzymes for corresponding pathways.

Supplementary Files

This is a list of supplementary files associated with this preprint. Click to download.

- SupplementaryInformation.docx